Analyst

MINIREVIEW

View Article Online
View Journal | View Issue

Cite this: *Analyst*, 2023, **148**, 1175

Paper-based microfluidics in sweat detection: from design to application

Zhichao Ye, †[b,e] Yuyang Yuan,†[a,b,e] Shaowei Zhan,[e,f] Wei Liu,[g] Lu Fang*[c] and Tianyu Li *[a,d]

Received 4th November 2022,
Accepted 15th February 2023

DOI: 10.1039/d2an01818g

rsc.li/analyst

Sweat, as a sample that includes a lot of biochemical information, is good for non-invasive monitoring. In recent years, there have been an increasing number of studies on *in situ* monitoring of sweat. However, there are still some challenges for the continuous analysis of samples. As a hydrophilic, easy-to-process, environmentally friendly, inexpensive and easily accessible material, paper is an ideal substrate material for making *in situ* sweat analysis microfluidics. This review introduces the development of paper as a sweat analysis microfluidic substrate material, focusing on the advantages of the structural characteristics of paper, trench design and equipment integration applications to expand the design and research ideas for the development of *in situ* sweat detection technology.

1 Introduction

Sweat is an important body fluid which plays a role in excretion and regulation of body temperature.[1,2] Being secreted by sweat glands, sweat is rich in electrolytes (Na^+, K^+, H^+, Ca^{2+}, *etc.*) and metabolic molecules (glucose, lactate, *etc.*),[3,4] which can be used to indicate the health status of the body at the molecular level.[5] In recent years, a number of groups have done research on related mechanisms, such as exploring the correlation between sweat analytes and blood analytes,[6–13] which drives the field of sweat analysis and analyte detection.[14] Notably, sweat can be collected in a non-invasive, continuous manner to provide the required sample for detection.[15,16] The distribution of exocrine sweat glands in various parts of the body is shown in Fig. 1a. The picture shows that exocrine sweat glands are distributed in almost all skin regions, which allows more options for the installation sites of wearable sweat analysis devices. Thus, the ideal wearing position for wearable sensors allows the collection and testing of body surface sweat without interfering with the wearers' daily activities.[17]

The rising research interest in sweat composition analysis has made sweat a potential biological sample for diagnostic purposes.[18] There are two main techniques for body surface sweat analysis: a non-*in situ* (*in vitro*) testing method and an *in situ* (body surface) testing method. Compared to *in vitro* sweat analysis techniques, *in situ* analysis of body surface sweat collects and detects sweat samples instantly at the location where the sweat is produced, avoiding the cumbersome sweat collection and pre-treatment. It also avoids the problem of requiring staff intervention during the analysis process and reduces the risk of sample contamination.[19] Along with the development of flexible electronics, continuous body surface sweat detection has been rapidly developed in recent years.

General wearable body surface sweat sensors are applied directly to the skin surface and measure sweat as soon as it is secreted. During prolonged measurement, the analyte crystals left after sweat evaporation near the electrode may dissolve again, resulting in changes in sweat marker concentration.[20,21] Sweat accumulation caused by prolonged measurements can block the sweat pores and cause subcutaneous edema, thus affecting the sweating rate.[22,23] Early studies on *in situ* detection of sweat on the body surface focused on the flexible, bendable aspects of the sensor substrate material, while often ignoring issues such as evaporation of sweat and mixing of old and new sweat due to sweat accumulation during continuous analysis.[4,24,25] These problems can directly affect the accuracy of on-body characterization. Despite the outstanding advan-

[a]*Department of Translational Medicine & Clinical Research, Sir Run Run Shaw Hospital, School of Medicine, Zhejiang University, Hangzhou 310028, China. E-mail: lty0127@zju.edu.cn*
[b]*Department of General Surgery, Sir Run Run Shaw Hospital, School of Medicine, Zhejiang University, Hangzhou 310028, China*
[c]*Department of Automation, Hangzhou Dianzi University, Hangzhou 310028, China. E-mail: fanglu@hdu.edu.cn*
[d]*National Engineering Research Center of Innovation and Application of Minimally Invasive Instruments, Sir Run Run Shaw Hospital, School of Medicine, Zhejiang University, Hangzhou 310028, China*
[e]*School of Medicine, Zhejiang University, Hangzhou 310028, China*
[f]*Department of Dermatology and Venereology, Sir Run Run Shaw Hospital, Zhejiang University School of Medicine, Hangzhou 310028, China*
[g]*College of Information Science and Electronic Engineering, Zhejiang University, Hangzhou 310028, China*
†These authors contributed equally to this work and share first authorship.

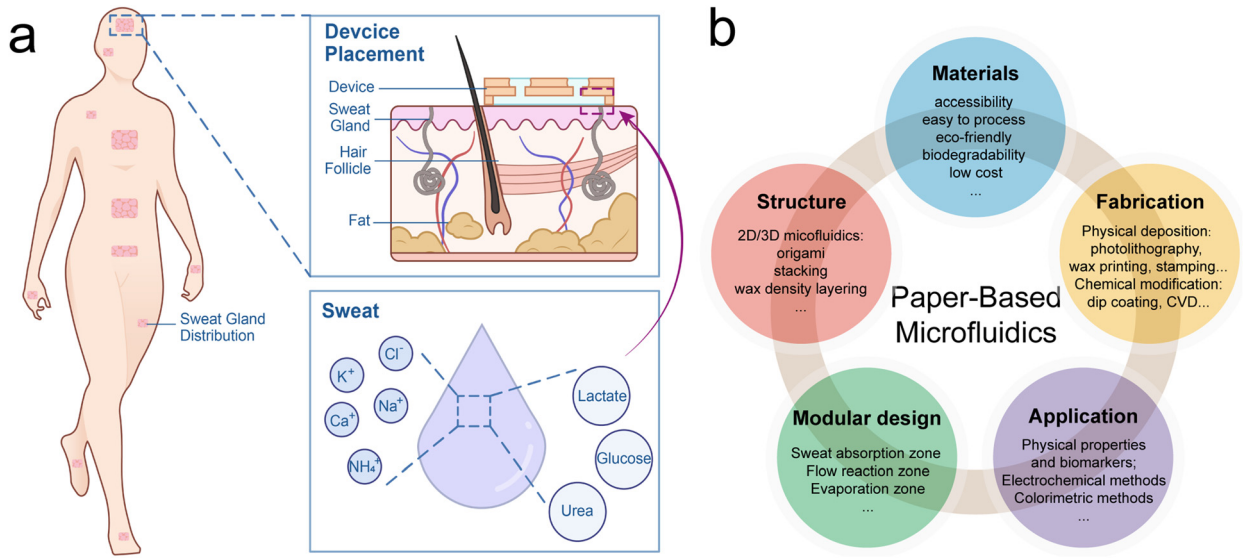

Fig. 1 (a) Distribution of sweat glands on the body surface, composition in sweat, and pattern diagram of sweat monitoring. (b) Key points of paper-based microfluidics.

tages of *in situ* sweat detection, there are still some problems in achieving reliable, non-invasive and real-time accurate detection.[5]

Recent studies have shown that microfluidic systems made of thin, soft materials with similar Young's modulus to that of skin can solve some of the problems mentioned above.[26,27] The structure of microfluidic systems needs to enable quick collection of sweat from the skin surface for subsequent sensing. Body surface sweat analysis devices based on colorimetric techniques can be integrated with microfluidic devices prepared from PDMS (polydimethylsiloxane) materials.[5,28] In the field of electrochemical body surface sweat analysis, the use of PDMS materials to prepare microfluidic devices for sweat collection and reactions has also been reported.[17,29] Although PDMS materials show some advantages in the preparation of body surface microfluidic systems, their preparation process is complex and costly (photolithography). Therefore, a material with low cost and a simple preparation process is required for mass production.[25]

Paper is considered an ideal substrate material for *in situ* sweat analysis because of its hydrophilicity, ease of processing, flexibility, low cost, environmental friendliness, and biocompatibility.[30] Recently, paper-based microfluidic devices have been developed for sweat collection and transport,[31,32] which benefits from hydrophobic treatment. In our previous study, we developed a three-dimensional paper-based microfluidic device by folding prefabricated cellulose paper for collecting sweat from the skin surface.[33,34] Thus, paper-based microfluidics have become a potential tool for *in situ* analysis of sweat to promote the development of healthcare management and exercise monitoring.[35,36]

As shown in Fig. 1b, this review focuses on the application and development of paper-based microfluidics in sweat detection. We first describe the structure and characteristics of paper and list a range of paper-based hydrophobic treatments for various needs. Then, the review discusses the structural design of the flow channel and the factors affecting the design of the microfluidics. Finally, the review summarizes the currently available equipment for *in situ* analysis of sweat based on paper substrates. Overall, the review provides an overview of the recent efforts in paper-based microfluidic devices and concludes by highlighting several challenges and envisioning new opportunities for *in situ* analysis of sweat.

2 Paper

Paper is a kind of material with a microscale porous network structure which mainly consists of cross-stacked and interconnected cellulose fibers.[37] The capillarity and hydrophilic ability of paper make it a pump-less alternative to generate microfluidics. Paper-based microfluidics can be precisely adjusted to meet various needs by varying various paper characteristics such as thickness, porosity, roughness, and wettability.[38–40] Patterned paper is ideal for low-cost, portable, and technically simple multiplexed bioassays.[41–44] Paper-based microfluidics offer many unique advantages over conventional microfluidics in terms of unpowered fluid transport *via* capillary action, high surface area to volume ratio for chemical reactions and assays, and the ability to store reagents in an active form within the fiber network.[45] With the advantages mentioned above, paper has become an attractive substrate material for *in situ* sweat detection, which makes it a promising starting point for a "lab on paper".

In the scientific community, we have come to accept the definition that a surface is hydrophobic when its static water contact angle θ is >90° and is hydrophilic when θ is <90°.[46]

The formula of Lucas–Washburn implies the relationship:

$$v = \frac{\gamma r \cos\theta}{4\eta L} = \frac{\mathrm{d}L}{\mathrm{d}t}$$

where v is the speed, γ is the surface tension, r is the radius, L is the length, η is the liquid viscosity, θ is the contact angle and t is the penetration time. For a certain paper type and a certain kind of liquid, L, γ and η can be considered as constant and v correlates with r as well as θ.

According to this formula, it is obvious that the capillary force can be modified by modifying the capillary radius and contact angle. For example, glue particles are fixed on the surface of the fiber and paper, covering part of the capillary or reducing the radius (r) of the capillary to reduce the penetration rate. The glue changes the surface properties of the paper, increases the interface contact angle (θ) between the paper surface and the liquid, and makes the paper obtain the ability to resist liquid penetration.[41]

As shown in Fig. 2, various fabrication techniques have been developed for microfluidics, mainly including wax-printing,[51] 2D shaping/cutting,[52] and 3D packaging/stacking.[53] Moreover, techniques of paper-based microfluidics such as photolithography, PDMS printing, inkjet etching, printed circuit, and plasma/laser treatment have also been developed quickly. According to the binding state of hydrophobic compounds and paper, we divide them into two categories: physical blockage and chemical modification. We classify common hydrophobic design according to these two categories.

In terms of physical blockage, photolithography is the first hydrophobic fabrication method used in paper-based microfluidics.[41] The success of wax printing has led to the development of fabrication methods enabling the creation of hemi- and fully enclosed channels within the paper.[42,54] Laser cutting and shaping makes paper thin and easy to fracture,[55] while the flexographic printing lacks reproducibility and flexibility.

In terms of chemical modification, covalent chemical modification of paper based on reacting with functional groups in cellulose is the most commonly used method.[56,57] For example, Malancha Gupta *et al.* demonstrated for the first time that solventless initiated chemical vapor deposition can be used for three-dimensional patterning of paper-based microfluidics with a thin layer of hydrophobic photo responsive poly(*o*-nitro benzyl methacrylate).[58] Hsiu-Yang Tseng *et al.* successfully developed programmable wicking profiles by alternating coated and uncoated zones with a solution composed of potassium alum and animal glue, which is a sizing material used in the fabrication of calligraphy Xuan paper.[59] Bahram Hemmateenejad *et al.* reported a three-dimensional origami paper-based analytical device (3D-mu PAD) for ABO and Rh blood type detection using a three-dimensional origami microfluidic technology, using alkyl ketene dimer (AKD) ink for hydrophobic design.[60] Chemical modification presents a more stable state whereas physical blocking, especially wax printing, shows great potential in manufacture.[61]

With the advantages of smooth surface, uniform structure, a high content of a-cellulose, and very good wicking properties,[62] Whatman No. 1 chromatography paper is the most-used paper substrate for paper-based microfluidics, while nitrocellulose paper is more widely used for lateral flow immunoassays[63,64] for its better protein adsorption ability.[65,66] As an alternative, office paper, a substrate of commercial interest, is accessible but less attractive for technical paper,[67,68] because the high amount of calcium carbonate ($CaCO_3$) present may interfere with the pH.[69] Using Whatman No. 1 chromatography paper, Mustafa Şen *et al.* demonstrated a paper-based microfluidic combined with a deep learning-based smartphone app called "DeepLactate" and then applied it for quantitative and selective determination of lactate concentration in sweat.[70] Whatman No. 4 is a very fast filtering paper with an excellent retention rate, whose size of pores is 20–25 μm and whose thickness is 210 μm.[71] Different combinations of different papers can also be formed. For example, Raquel B. R. Mesquita *et al.* described a paper-based microfluidic for the quantification of total phenolic compounds in wines with the top layer consisting of 24 papers (Whatman® 541, pore size 20–25 μm, thickness 160 μm) and the bottom layer consisting of 24 papers (Whatman® 3, pore size 6 μm, thickness 390 μm).[40]

In summary, paper is known as an interlaced network of cellulose fibers that wicks fluids by capillarity. As a kind of hydrophilic and pump-less material, which is discussed when talking about its advantages, paper is extremely suitable to generate microfluidics. Various hydrophobic fabrications of paper summarized above optimize the design of microfluidics furthermore. In addition, different kinds of paper listed in this part can meet different needs when applied in paper-based microfluidics. Taking all these factors into consideration, paper can be an extraordinary candidate substrate for microfluidics in flexible and wearable devices.

3 The structure of paper-based microfluidics

3.1 2D paper-based microfluidics

The application of paper as substrate materials for the sensing field has a long history. In 1949, Ralph H. Müller and Doris L. Clegg designed a patterned filter paper to speed up the diffusion process and to minimize the sample volume.[72] It was recognized as the prototype of paper-based microfluidics. For decades, paper has been used as a platform of analytical chemistry, such as chromatography,[73–75] immunoassay,[76–78] electrochemical analysis[79–82] *etc*. With the development of a variety of techniques of hydrophobic boundaries, such as wax printing,[83] photolithography,[84] and plasma treatment,[85,86] the hydrophobic and hydrophilic zones of the microfluidics are clearly demarcated so that the paper acts not only as a platform, but also as a flow channel to guide the liquid flow, which allows it to be used in a wider range of applications in sensing.

In 2007, George M. Whitesides *et al.* used photolithography to pattern photoresist (SU-8, SC) embedded in paper and

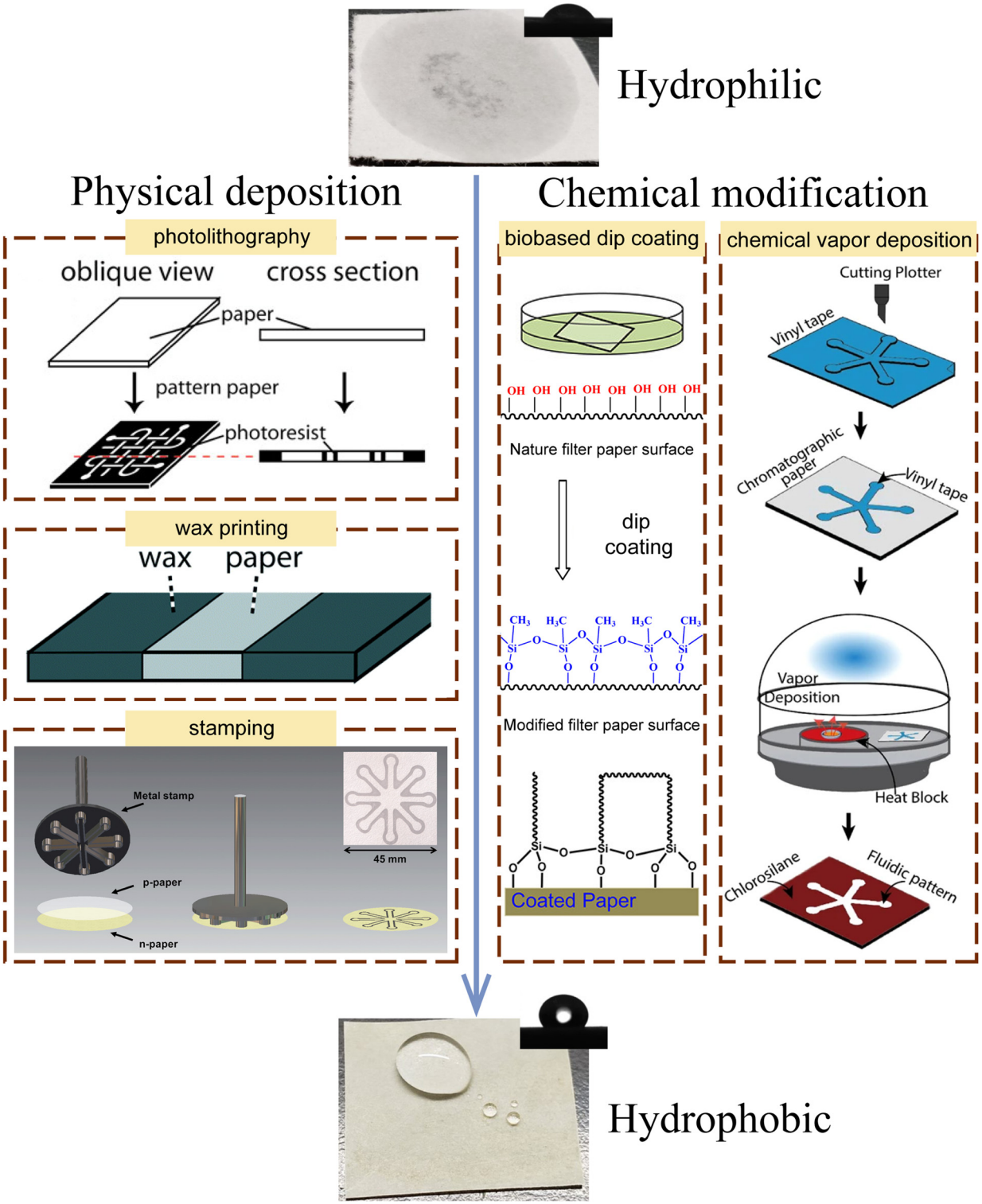

Fig. 2 Various fabrication techniques including physical deposition and chemical modification. Adapted and reproduced with permission from ref. 45–48. Copyright 2008 National Academy of Science, 2014 The Royal Society of Chemistry, 2015 The Royal Society of Chemistry, 2018 Elsevier B.V, 2019 American Chemical Society.[47–50]

designed a 2D paper-based microfluidic to confine liquid flow within the channel in a controlled manner, which was used for the determination of glucose and protein in artificial urine.[41] It was regarded as the first 2D paper-based microfluidic for inspection in liquid flow. 2D paper-based microfluidics are simple to design and fabricate, which realizes the function

of collecting and conducting sweat on the body surface. Since then, a growing number of research studies in paper-based microfluidics have sprung up, mainly focusing on the methods of hydrophobic modification,[51,87] the design of microfluidic structure[52,88–93] and application in biosensors.[79,80,94–97]

The geometry and size of the 2D paper-based microfluidics play critical roles in the fluid flow of microfluidic devices. The width of the channel affects the speed of liquid flow. As shown in Fig. 4b, a decrease in channel width can increase wicking speed.[93] Details on this part will be discussed in later sections. As a result, fan-shaped[98,99] and dendritic[33,100] microfluidics had emerged, different from traditional rectangular designs.

However, 2D microfluidics have limitations in complex fluidic manipulations. For example, it is hard for 2D microfluidics to realize sample pre-treatment or multi-parameter detection in the same occupied area.[104–106]

3.2 3D paper-based microfluidics

Compared to 2D paper-based microfluidics, 3D paper-based microfluidics offer more dimensions to facilitate the design of structures. It allows more complex detection and analysis processes to be performed on a single platform to integrate more functions, thus developing the potential of multi-step detection in a compact device.[107] In 2008, George M. Whitesides *et al.* designed a filter paper-based 3D microfluidic analysis device for the determination of glucose and proteins in artificial urine,[47] which was regarded as the first analysis device based on 3D microfluidics. As Fig. 3d shows, the microfluidic drives the fluid from the top four inputs to the bottom 1024 output detection points. Such a structural design allowed the fluid to flow laterally within each layer, or vertically between layers, which minimized the quantity of sample loss and decreased the required sample volume. This device presents a feasible solution for subsequent high-throughput analysis of paper-based microfluidics.

While the 3D structure has many advantages over the 2D ones, the difficulty in designing the 3D structure lies in achieving the connection of the hydrophilic zone between the layers.[108] This is the transformation process from a flat hydrophobic structure to a three-dimensional hydrophobic structure. Recent studies have explored hydrophobic design methods for vertical structures, which mainly include the following forms. First, stacking of two-dimensional paper-based microfluidics with multiple sheets of paper is an easy way to produce 3D paper-based microfluidics. For example, Frank A. Gomez *et al.* demonstrated a glucose detection platform based on 3D stacked paper-based microfluidics in 2019.[109] In addition, the researchers introduced the idea of valve switching in traditional microfluidics into paper and fabricated paper-based microfluidics with a switching function. For example, Chaoyong James Yang *et al.* demonstrated an "on and off" paper-based microfluidic.[102] As Fig. 3f shows, the formation of hydrogels overcame the capillary force, preventing the dye solution from flowing further. Using an aptamer as a cross-linker, a smart, target-responsive hydrogel can be synthesized, in which target binding can mediate gel–sol phase switching. As a result, the corresponding dye colour will appear in the responsive circles. Second, origami of two-dimensional paper-based microfluidics is another way to produce 3D paper-based microfluidics, which achieves the integration of paper-based microfluidics on a single sheet of paper.[110] For example, Jinghua Yu *et al.* demonstrated a multiplexed chemiluminescence immunoassay for point-of-care diagnostics based on 3D origami-based microfluidics in 2012.[101] Third, wax density layering for single paper is a novel method for 3D paper-based microfluidic construction, which achieved fabrication without folding. As Fig. 3g shows, Xiao Li *et al.* created microfluidics in single sheets of paper by controlling the density of deposited wax on paper.[103]

3.3 Modular design

A microfluidic system typically consists of many different modules, such as reaction chambers, mixers, detectors, pumps, valves, *etc*.[111] Benefiting from the capillary force, paper-based microfluidics provide a pump-less alternative to generate microfluidics.[112,113] The key to using paper-based microfluidics for *in situ* monitoring lies in modular design. The most important of these are the sweat absorption buffer zone, the flow reaction zone, and the evaporation zone.

The function of the sweat absorption buffer zone is to absorb sweat from the skin surface. Scallop or vortex shapes are the most common shapes of the sweat absorption buffer zone, which aim to pursue efficient sweat absorption. For example, Chengyi Hou *et al.* demonstrated a vortex shaped one in 2021.[114] The results showed that the sweat diffusion rate in layer 1 was very fast in the first 5 seconds, which reflected the high efficiency of the vortex shape for sweat absorption and transfer. In addition, the diffusion rate of sweat decreased layer by layer, indicating that the hydrophilic region of each layer has a buffering effect on the next layer. Notably, the sweat absorption buffer zone stabilized the diffusion rate of sweat on the next functional layer, which is essential to avoid fluctuations in electrical signals during real-time monitoring. Parallel results, during a review of research in recent years, were found in which Qingpeng Cao *et al.*[33] and Tianyu Li *et al.*[100] all designed multilayer structures, realizing efficiency of sweat absorption.

The capillary flow rate is a key parameter in the performance of the assay in the flow reaction zone due to the fact that the effective concentration of the analytes is related to the capillary flow rate.[115,116] Ever since its empirical formulation in 1856, Darcy's law has been a hallmark in modelling momentum transport through porous media.[117] In 2010, Jennifer L. Osborn *et al.* focused on the flow in conventional paper-based microfluidic ducts.[112] Assuming the sample pad is an infinite source and the absorbent pad is an infinite sink, the flow in a fully wetted paper device is approximated by Darcy's law:

$$Q = \frac{\kappa w h}{\mu L} \Delta P$$

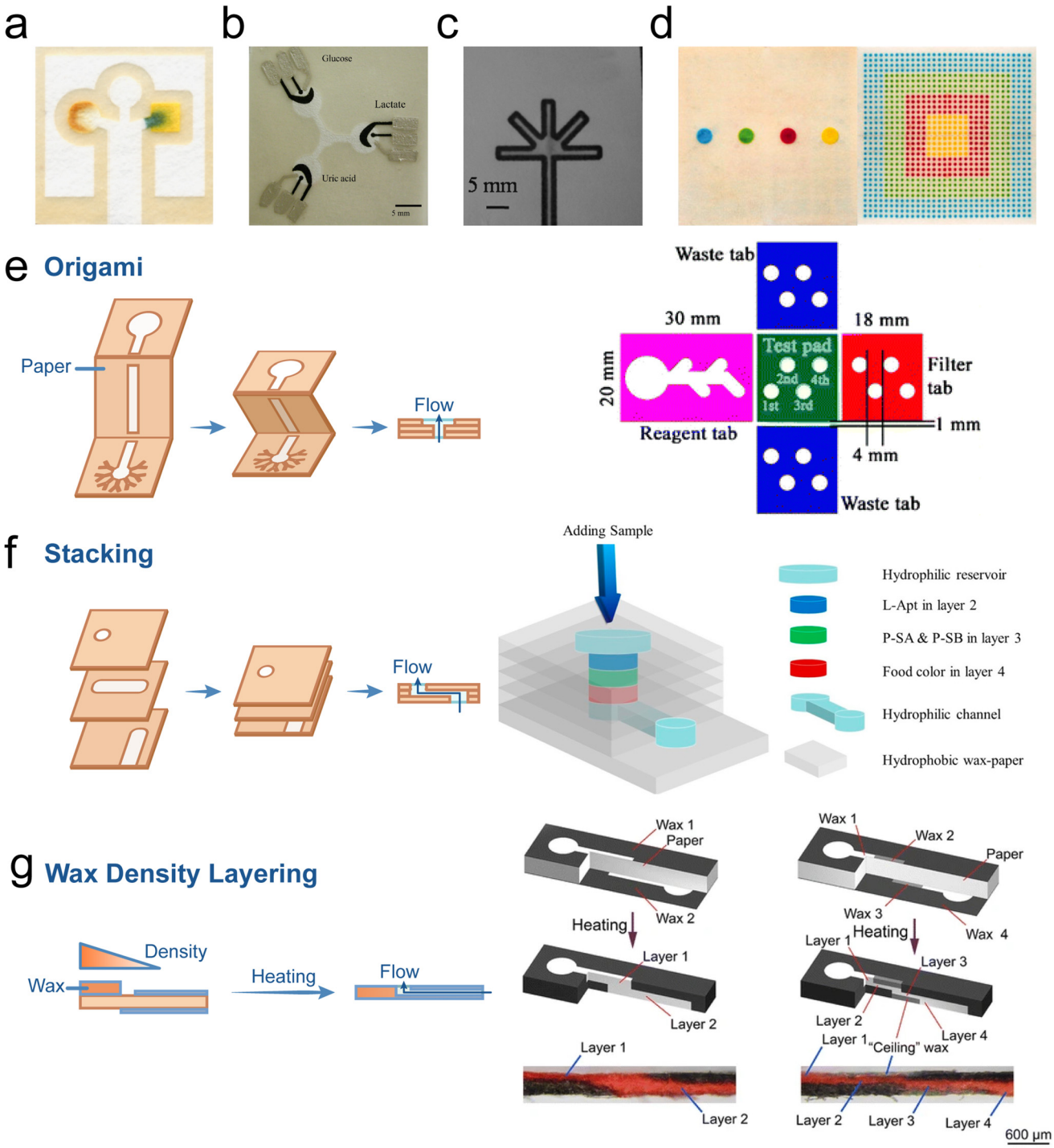

Fig. 3 Typical 2D/3D paper-based microfluidics. (a) The first 2D paper-based microfluidic. Reproduced with permission from ref. 38. Copyright 2007 WILEY-VCH.[41] (b) The first 2D paper-based microfluidic used for electrochemical detection. Reproduced with permission from ref. 72. Copyright 2009 American Chemical Society.[79] (c) A typical dendritic 2D paper-based microfluidic. Reproduced with permission from ref. 27. Copyright 2009 WILEY-VCH.[88] (d) The first 3D paper-based microfluidic.[47] (e) A 3D origami paper-based microfluidic. Reproduced with permission from ref. 38. Copyright 2012 The Royal Society of Chemistry.[101] (f) A 3D stacking "on and off" paper-based microfluidic. Reproduced with permission from ref. 39. Copyright 2015 American Chemical Society.[102] (g) A wax density layering 3D paper-based microfluidic. Reproduced with permission from ref. 40. Copyright © 2014 Springer-Verlag Berlin Heidelberg.[103]

where Q is the volumetric flow rate, κ is the permeability of the paper, wh is the paper cross-sectional area of width, w, and height, h, μ is the dynamic viscosity, and ΔP is the pressure drop occurring over the length, L, of the paper network. Due to this, it is possible to change the volumetric flow rate Q controlled by simply changing the fluid path length, fluid path

diameter, fluid depth, and thickness. The patterning process defines the width and length of paper-based microfluidics, and the thickness of the paper defines the height of the channel.

This assumption is correct when the effect of the evaporation process in paper-based microfluidics is not taken into account. However, due to the need of continuous monitoring, the effect of the evaporation process plays a significant role. In that case, the mass of the evaporated water per unit time equals the mass flow rate through the channel, when the device is completely saturated with water. In 2020, Orlin D Velev *et al.* incorporated the retardation factor and rearranged the equation result in an expression for dye velocity.[118]

$$v = \frac{R_f HA}{wM}$$

where v is velocity, R_f is the retardation factor of the paper, HA is the constant evaporation flux, H, and the area of the evaporation zone, A, M is moisture content of the wet paper, w is the channel width. Therefore, the flow rate can be changed by changing the channel width and evaporation area. However, the areas of the evaporation zone lie below the line in Fig. 4c.[118] Otherwise, the evaporation zone will be not fully saturated, since the capillary wicking is not able to replenish water rapidly enough to fully saturate the pad area. In this case, the flow should be described according to Darcy's law. Therefore, assessment of the evaporation area is crucial. Attention should be paid to whether the flow reaction area is incorporated into the evaporation area and whether it is obscured by encapsulation.

With the development of integrated equipment and the demand for multi-parameter detection, 3D paper-based microfluidics are becoming the future development trend step by step.[33,100,119] However, most of the previous research studies have focused on a single layer, and there is a lack of evidence in the research between layers currently. Vertical flow in paper may need further investigation, for which diagnostic devices based on vertical sample flow are possible.[114] Since an external driving force is not necessary for paper-based microfluidics, we did not include it in this paper.

4 Paper-based microfluidic devices for *in situ* sweat analysis

In situ sweat analysis devices are booming with the development of flexible and conductive materials with good performance.[120] As discussed above, paper, to some extent, is a cost-effective substitute for PDMS as a detection module and paper-

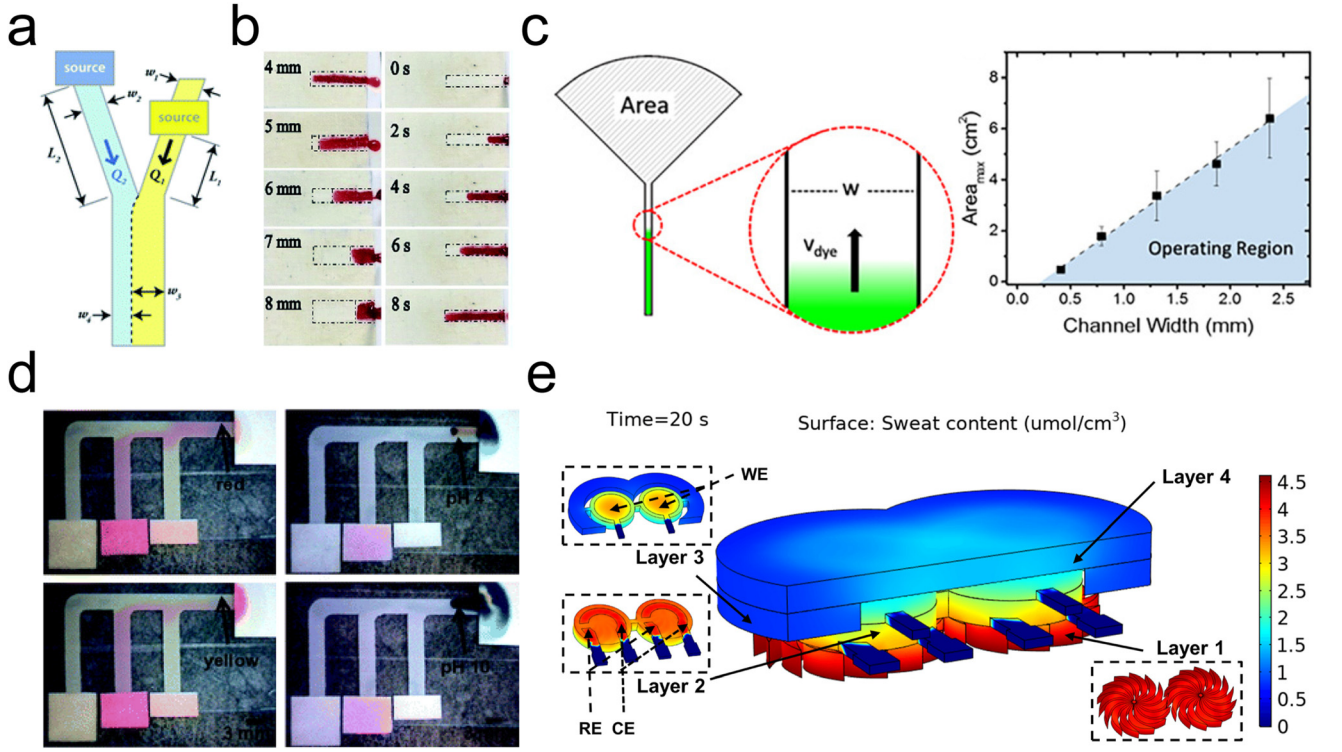

Fig. 4 Research studies in the flow regime of 2D/3D paper-based microfluidics. (a) A schematic of the paper Y device for validating Darcy's law. Reproduced with permission from ref. 5. Copyright 2010 The Royal Society of Chemistry.[112] (b) The relationship of channel width and wicking speed. Reproduced with permission from ref. 6. Copyright 2019 The Royal Society of Chemistry.[93] (c) A typical dendritic 2D paper-based microfluidic. Reproduced with permission from ref. 19. Copyright 2020 American Institute of Physics.[118] (d) Demonstration of programmed fluid delivery using a simple 2D paper network. Reproduced with permission from ref. 23. Copyright 2010 The Royal Society of Chemistry.[90] (e) Dynamic distribution of sweat contents in a 3D paper-based microfluidic. Reproduced with permission from ref. 21. Copyright 2020 Elsevier B.V.[114]

based microfluidics economically solves the long-standing headaches caused by undesired sweat accumulation and contamination in *in situ* sweat analysis. Along with the insights from research studies on effective channel design, there are a growing number of outcomes regarding paper-based microfluidic devices for versatile applications. These devices employ different principles to evaluate the sweat loss[121–123] and detect chemical molecules such as electrolytes,[97,119,122] small molecules[124–126] and major molecules[127] in sweat. This review is a retrospect on the paper-based microfluidic devices reported previously for *in situ* sweat analysis sorted by different detecting objects.

Monitoring the physical properties of sweat such as the perspiration volume and rate is vital for assessing physiological status and improving athletic performance[20,128–130] and correction for biomarker measurement in sweat.[26,29,123,131] Some previous works have reviewed the research progress in wearable sweat-loss measuring devices[132] while this section focuses more on the application of paper-based microfluidic devices in this field. Due to the hygroscopicity or capillarity, paper-based microfluidic devices facilitate the channel with self-driving ability. This unique property endows paper-based microfluidic devices with extraordinary advantages over other microfluid devices. Andreu Vaquer *et al.* developed a sweat volume colorimetric platform made of filter paper.[123] The absorbed sweat was dyed after passing through the dye reservoir on the filter paper, leaving a path on the paper strip. The length of the colour band quantitatively reflected the sweat volume. Though simple in design and intuitive in results, it failed to manifest the change of sweat volume over time, and the uneven diffusion of the dye front could likely cause reading errors. Vaibhav Jain *et al.* realized time sampling by constructing a 2D paper-based radial microfluidic array using a colorimetric method to demonstrate sweat dynamics.[121] The device consisted of a series of microfluidics with different lengths and widths which were designed to allow the collected sweat to flow at the same rate. The blue $CoCl_2$ deposited at the end of the channel turned red when it was hydrated as $CoCl_2{\cdot}6H_2O$. Therefore, the number of channels that turned red semi-quantitatively and semi-continuously reflected the perspiration dynamics.

Colorimetric and electrochemical methods are mainly used for sweat-loss evaluation.[132] However, only the colorimetric method was reported in paper-based microfluidic devices. Colorimetry was the most traditional application of filter paper, which was featured as simple and intuitive. Unfortunately, it was incapable of continuous monitoring.[121,123] With the development of flexible conductive paper-based composite materials,[136] it is promising to combine electrochemical methods with paper-based microfluidic devices in the future to realize continuous monitoring of perspiration volume and rate.

Table 1 Advantages and disadvantages of various paper-based microfluidic integrated devices

Detection methods	Device	Target	Limit of detection	Advantages	Disadvantages	Ref.
Electrochemical	Wax printing 3D paper-based microfluidic electrochemical integrated device	Glucose	5 μM	1. Continuous monitoring in real time	1. Difficult to manipulate	33
		Glucose	10.3 μM	2. Quantitative detection	2. Complex fabrication process	100
		Glucose	17.05 μM	3. High detection sensitivity and low limit of detection	3. Low mechanical properties	114
		Lactate	3.73 μM	4. Environment-friendly, biodegradable and low cost		133
	Office paper-based electrochemical sensor	Zn(II)	25 ng mL^{-1}			
	PDMS-based microfluidic patch	Glucose	7.34 μM	1. Skin-compatible mechanical properties	1. Surface adsorption	134
		Lactate	1.24 mM	2. Versatility and rapid prototyping	2. Heat does not dissipate easily	
					3. Relatively high cost	
Colorimetric	Chemically patterned microfluidic paper-based analytical device	Glucose	13 mg dL^{-1}	1. Easy to manipulate	1. No capacity for continuous monitoring	50
		TNFα	3 ng mL^{-1}	2. Usually simple fabrication process	2. Usually qualitative detection	
		Ni	150 μg L^{-1}	3. Environment-friendly, biodegradable and low cost	3. Low mechanical properties	
	Wax printing 3D paper-based microfluidic electrochemical integrated device	Glucose	—			122
		Lactate	—			
		pH	—			
	2D paper-based microfluidic analytical device	pH	—			125
		Urea	—			
	3D paper-based microfluidic analytical device	BSA	—			127
		Glucose	—			
	PDMS-based colorimetric sensing device with super absorbent polymer valves	Chloride	1 mM	1. Skin-compatible mechanical properties	1. Surface adsorption	135
				2. Biocompatible and profoundly precise	2. Heat does not dissipate easily	
					3. Relatively high cost	

Sweat is rich in electrolytes and chemical substances, among which, Cl^- concentration is an important indicator for the diagnosis of cystic fibrosis[137,138] and levels of Na^+, K^+, H^+ well reflect the body dehydration state.[139–141] Furthermore, given that lactate concentration in sweat and blood are highly correlated, lactate in sweat well reflects the degree of muscle fatigue.[32] Sweat glucose is also an important pointcut for non-invasive body glucose level monitoring,[9] which has captured extensive attention.[20,142] As shown in Table 1, many research studies successfully applied colorimetric and electrochemical methods in the *in situ* detection of analytes with paper-based microfluidic devices. Colorimetry is widely used to detect sweat pH,[97,122] lactate,[32,125] glucose,[127] creatinine,[125] uric acid,[125] protein content,[127] *etc*. As shown in Fig. 5a, Zhong Zhang *et al.* designed a multifunctional paper-based microfluidic colorimetric device that simultaneously measured the sweat volume, pH and lactate and glucose content.[122] Patterned filter paper separated the detection area as different functional regions. pH indicator solution, L-lactate oxidase/horseradish peroxidase/*o*-phenylenediamine dihydrochloride

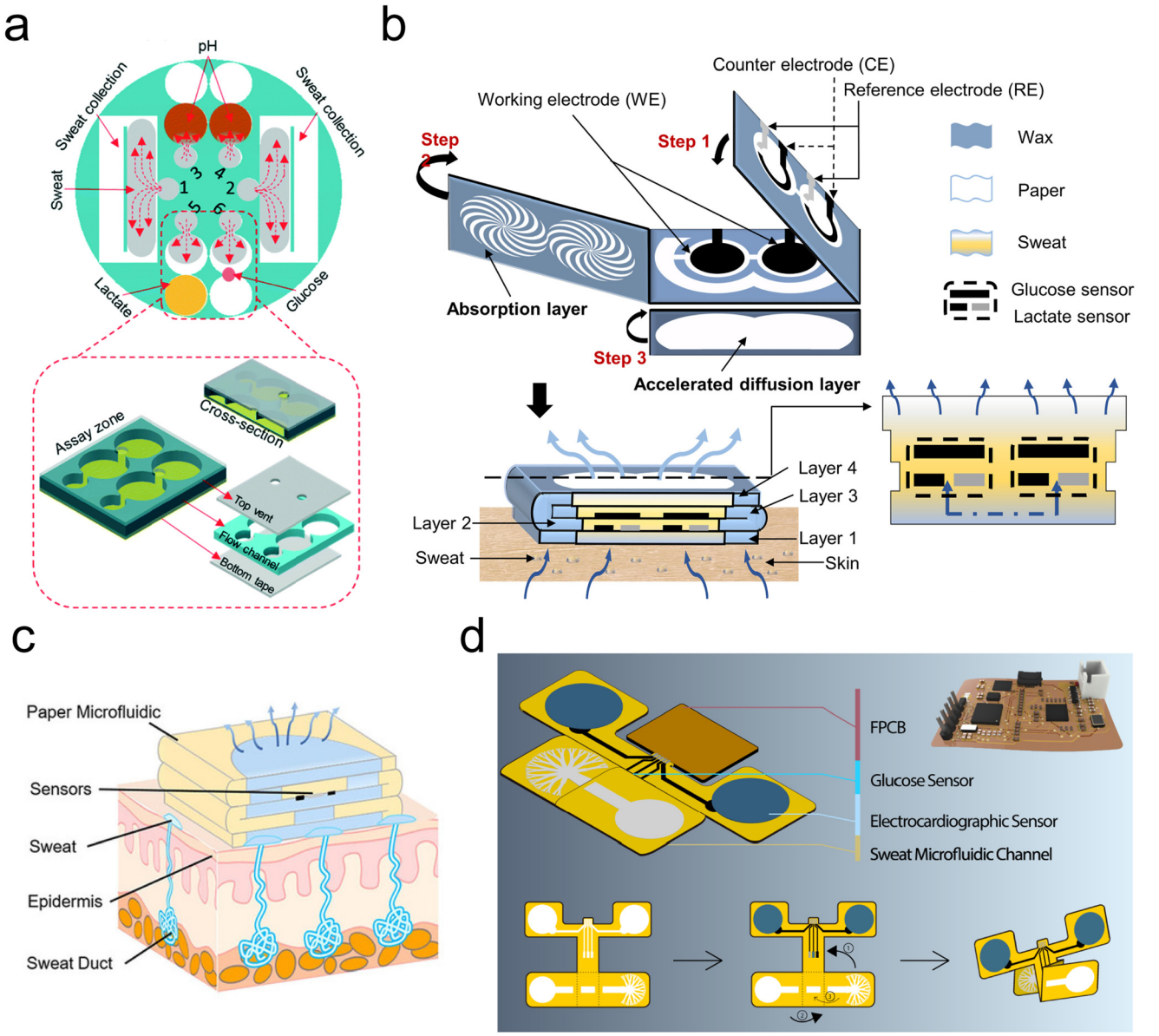

Fig. 5 Typical paper-based microfluidics for sweat content measurement. (a) A 3D device by stacking, for versatile applications using a colorimetric method. Reproduced with permission from ref. 8. Copyright 2019 The Royal Society of Chemistry.[122] (b) A 3D device by origami featured with integrated processing of electrodes and channels. Reproduced with permission from ref. 9. Copyright 2021 Elsevier B.V.[100] (c) A 3D device by origami, for sweat electrolyte electrochemical monitoring. Reproduced with permission from ref. 20. Copyright 2020 Wiley-VCH.[119] (d) A 3D device by origami with a unique vortex-like absorption layer to accelerate sweat absorption. Reproduced with permission from ref. 21. Copyright 2020 Elsevier B.V.[114]

(OPD), and glucose oxidase/horseradish peroxidase/AAP/DHBS were respectively modified on functional regions to detect pH, lactate and glucose concentration. Chromogenic intensities were quantified using smartphone photography and ImageJ software processing. However, the double conversion from analyte concentration to colour intensity, and then to the image analysis software magnified the error.

Electrochemical methods have been widely used in *in situ* sweat monitoring because of their high sensitivity, dynamic recording and ease of miniaturization.[16] Several research groups reported their work on paper-based microfluidic devices for *in situ* sweat electrochemical monitoring, which performed well in the detection of sweat glucose[33,100,124] and lactate.[114] Qingpeng Cao *et al.* and Jiawang Ding *et al.* designed 3D paper-based microfluidic devices for potentiometric biosensing on enzyme activities and electrolyte level.[110,119] In Cao's work, the paper-based microfluidic device includes five layers, namely sweat collector layer, vertical channel layer, lateral channel layer, electrode layer, and sweat evaporator layer.[119] The 3D structure was constructed by folding, in which Na^+ and K^+ selective electrodes were attached to the electrode layer using double-sided tape to respond to the change in sweat Na^+ and K^+ concentration. This work also integrated a paper-based microfluidic device with a smartwatch, and results demonstrated that the device successfully solved the problem of sweat accumulation and exhibits desirable performance in both *in vivo* and *in vitro* tests. For glucose detection, Tianyu Li *et al.* also used origami to construct 3D paper-based microfluidic devices, but they made important improvements to the fabrication and design of the device.[100] As shown in Fig. 5c, the research group realized the integrated processing of electrodes and channels by screen printing technology. Moreover, a dendritic absorption area was designed to improve the efficiency of sweat collection and conductive hydrogel material was used to construct a glucose electrode, which contributed to an unprecedented high sensitivity for glucose detection. The device integrated the absorption area, ECG electrode, glucose detection electrode, and evaporation area on a single filter paper, realizing non-invasive real-time monitoring of electrophysiological and biochemical signals with low cost and high efficiency. Similar work was done by Li *et al.*[114] Notably, they designed a unique vortex structure to accelerate the absorption and transduction of sweat, which was proved to be effective by the simulation analysis of dynamic distribution of sweat diffusion. In conclusion, paper-based microfluidic electrochemical devices have great potential for *in situ* detection of sweat components, but there is still a problem of low device integration.

5 Conclusions and perspective

With the advantages of accessibility, ease of processing, environment-friendliness, biodegradability and low cost, paper became an attractive substrate material for *in situ* sweat detection, which makes it a promising starting point for a "lab on paper".

This paper reviewed the advantages of paper as an ideal candidate substrate material for microfluidics and summarized the up-to-date research progress on *in situ* sweat detection. Firstly, we described the two intrinsic characteristics of paper—hydrophilic property and capillary action based on the structure of paper—and presented an overview of the different methods of hydrophobic treatment to realize the functionality of paper-based microfluidics. Next, we introduced some classic 2D/3D structures of paper-based microfluidics and the basic concepts of dynamics of fluids in porous media. Finally, we presented some integrated devices for *in situ* sweat detection based on paper-based microfluidics. Here are some summaries and outlook from the review.

In terms of the design of paper-based microfluidics, the following recommendations are summarized:

(1) Choice of the paper type. Different types of paper show different characteristics, such as weight, thickness, porosity, particle retention, filtration speed, and wicking speed, making it possible to meet various needs. For example, with bigger porosity and faster wicking speed, Whatman #4 paper is a better choice for a microfluidic substrate.

(2) Choice of the hydrophobic method. Chemical modification presents a more stable state whereas physical blocking, especially wax printing, shows great potential in manufacture.

(3) The co-design of channel module and size. Paper-based microfluidics consist of a sweat absorption buffer zone, the flow reaction zone, and the evaporation zone, in which the flow rate of the flow reaction zone plays an important role in *in situ* sweat detection. The size of the channel, especially its width and evaporation area, is relevant to the flow rate.

Although paper-based microfluidics have been in development for more than a decade, there are still many key challenges remaining to be overcome during *in situ* sweat detection as described below.

(1) Salt deposition problem during long-term monitoring: While the water in the sweat is evaporated, it leaves behind dry salt deposits, which will hinder the operation of the equipment over time.

(2) Paper wetting problem during long-term monitoring: Whether chemically modified or physically blocked, the hydrophobized paper has a certain shelf life, which imposes limitations on long-term *in situ* sweat detection.

(3) Minimizing the structure of the microfluidics: Although 3D paper-based microfluidics have made some progress compared with 2D ones, there is still room for further improvement in integrating more functions in less space.

In recent years, we have witnessed the beginning of paper-based integrated analytical devices. The iterations of these sensing devices depend on the developments of advanced functional materials, which have made a splash in recent years including nanoparticles,[143] hydrogels,[100] aerogels,[144,145] and so on. In particular, conductive materials, such as PEDOT:PSS,[146] carbon nanotubes,[147] polyaniline (PANI),[148] and MXene (Ti3C2),[149] play an important role in sensors.[150] Their

development has led to optimization for device miniaturization and detection sensitivity.[151] Beyond doubt, progress in materials will foster the development of paper-based integrated analytical devices aimed at *in situ* sweat detection.

In summary, this review presents the recent advancements in paper-based microfluidics related to design and applications. The challenges associated with the device are also discussed and future directions are provided. It is hoped that this review will accelerate the development of a lab on paper in the field of *in situ* sweat detection.

Author contributions

YZC, YYY, and ZSW wrote the manuscript. LW contributed to the project planning. LTY and FL conceived, designed, and oversaw the project, and revised the manuscript. All the authors have discussed and commented on the manuscript.

Conflicts of interest

There are no conflicts to declare.

Acknowledgements

We thank the study participants for their time and effort. We thank Zhe Chen for her contribution in graphic design. We thank Professor Xuesong Ye's team for their contribution to research of paper-based microfluidics in sweat detection. We gratefully thank the National Natural Science Foundation of China, China (82272120), Natural Science Foundation of Zhejiang Province, China (LTGG23H180001, LQ20F010011, LY18H180006), and Key Research and Development Program of Zhejiang Province, China (2022C03002).

References

1 C. L. Tan and Z. A. Knight, *Neuron*, 2018, **98**, 31–48.
2 Y. Lu, Y. Fujita, S. Honda, S. H. Yang, Y. Xuan, K. Xu, T. Arie, S. Akita and K. Takei, *Adv. Healthc. Mater.*, 2021, **10**, e2100103.
3 S. J. Montain, S. N. Cheuvront and H. C. Lukaski, *Int. J. Sport Nutr. Exercise Metab.*, 2007, **17**, 574–582.
4 W. Gao, S. Emaminejad, H. Y. Y. Nyein, S. Challa, K. V. Chen, A. Peck, H. M. Fahad, H. Ota, H. Shiraki, D. Kiriya, D. H. Lien, G. A. Brooks, R. W. Davis and A. Javey, *Nature*, 2016, **529**, 509–514.
5 M. Bariya, H. Y. Y. Nyein and A. Javey, *Nat. Electron.*, 2018, **1**, 160–171.
6 J. M. Green, P. A. Bishop, I. H. Muir, J. R. McLester and H. E. Heath, *Int. J. Sports Med.*, 2000, **21**, 556–560.
7 I. Alvear-Ordenes, D. Garcia-Lopez, J. A. De Paz and J. Gonzalez-Gallego, *Int. J. Sports Med.*, 2005, **26**, 632–637.
8 D. A. Sakharov, M. U. Shkurnikov, M. Y. Vagin, E. I. Yashina, A. A. Karyakin and A. G. Tonevitsky, *Bull. Exp. Biol. Med.*, 2010, **150**, 83–85.
9 J. Moyer, D. Wilson, I. Finkelshtein, B. Wong and R. Potts, *Diabetes Technol. Ther.*, 2012, **14**, 398–402.
10 M. Gamella, S. Campuzano, J. Manso, G. G. de Rivera, F. Lopez-Colino, A. J. Reviejo and J. M. Pingarron, *Anal. Chim. Acta*, 2014, **806**, 1–7.
11 J. Kim, I. Jeerapan, S. Imani, T. N. Cho, A. Bandodkar, S. Cinti, P. P. Mercier and J. Wang, *ACS Sens.*, 2016, **1**, 1011–1019.
12 L. B. Baker, *Sports Med.*, 2017, **47**, S111–S128.
13 X. Xuan, C. Pérez-Ràfols, C. Chen, M. Cuartero and G. A. Crespo, *ACS Sens.*, 2021, **6**, 2763–2771.
14 M. Q. Wang, Y. R. Yang, J. H. Min, Y. Song, J. B. Tu, D. Mukasa, C. Ye, C. H. Xu, N. Heflin, J. S. McCune, T. K. Hsiai, Z. P. Li and W. Gao, *Nat. Biomed. Eng.*, 2022, **6**, 1225–1235.
15 J. Choi, R. Ghaffari, L. B. Baker and J. A. Rogers, *Sci. Adv.*, 2018, **4**, eaar3921.
16 J. Kim, A. S. Campbell, B. E. F. de Avila and J. Wang, *Nat. Biotechnol.*, 2019, **37**, 389–406.
17 S. B. Kim, K. Lee, M. S. Raj, B. Lee, J. T. Reeder, J. Koo, A. Hourlier-Fargette, A. J. Bandodkar, S. M. Won, Y. Sekine, J. Choi, Y. Zhang, J. Yoon, B. H. Kim, Y. Yun, S. Lee, J. Shin, J. Kim, R. Ghaffari and J. A. Rogers, *Small*, 2018, **14**, 1802876.
18 N. Brasier, M. Osthoff, F. De Ieso and J. Eckstein, *J. Med. Internet Res.*, 2021, **23**, e25907.
19 Y. X. Zhang, Y. Chen, J. L. Huang, Y. C. Y. Liu, J. F. Peng, S. D. Chen, K. Song, X. P. Ouyang, H. Y. Cheng and X. F. Wang, *Lab Chip*, 2020, **20**, 2635–2645.
20 A. J. Bandodkar, W. J. Jeang, R. Ghaffari and J. A. Rogers, *Annu. Rev. Anal. Chem.*, 2019, **12**, 1–22.
21 R. Ghaffari, J. A. Rogers and T. R. Ray, *Sens. Actuators, B*, 2021, **332**, 129447.
22 D. F. Brebner and D. M. Kerslake, *J. Physiol.*, 1964, **175**, 295–302.
23 C. E. Dziedzic, M. L. Ross, G. J. Slater and L. M. Burke, *Int. J. Sports Physiol.*, 2014, **9**, 832–838.
24 H. Y. Y. Nyein, W. Gao, Z. Shahpar, S. Emaminejad, S. Challa, K. Chen, H. M. Fahad, L. C. Tai, H. Ota, R. W. Davis and A. Javey, *ACS Nano*, 2016, **10**, 7216–7224.
25 G. Xu, C. Cheng, Z. Y. Liu, W. Yuan, X. Z. Wu, Y. L. Lu, S. S. Low, J. L. Liu, L. H. Zhu, D. Z. Ji, S. Li, Z. T. Chen, L. S. Wang, Q. G. Yang, Z. Cui and Q. J. Liu, *Adv. Mater. Technol.*, 2019, **4**, 1800658.
26 Z. Sonner, E. Wilder, J. Heikenfeld, G. Kasting, F. Beyette, D. Swaile, F. Sherman, J. Joyce, J. Hagen, N. Kelley-Loughnane and R. Naik, *Biomicrofluidics*, 2015, **9**, 031301.
27 R. Ghaffari, J. Choi, M. S. Raj, S. Chen, S. P. Lee, J. T. Reeder, A. J. Aranyosi, A. Leech, W. H. Li, S. Schon, J. B. Model and J. A. Rogers, *Adv. Funct. Mater.*, 2020, **30**, 1907269.
28 T. Ray, J. Choi, J. Reeder, S. P. Lee, A. J. Aranyosi, R. Ghaffari and J. A. Rogers, *Curr. Opin. Biomed. Eng.*, 2019, **9**, 47–56.

29 Z. Yuan, L. Hou, M. Bariya, H. Y. Y. Nyein, L. C. Tai, W. B. Ji, L. Liabc and A. Javey, *Lab Chip*, 2019, **19**, 3179–3189.
30 T. Akyazi, L. Basabe-Desmonts and F. Benito-Lopez, *Anal. Chim. Acta*, 2018, **1001**, 1–17.
31 F. Figueredo, P. T. Garcia, E. Corton and W. K. T. Coltro, *ACS Appl. Mater. Interfaces*, 2016, **8**, 11–15.
32 M. Saha, *Oper. Matrices*, 2021, **15**, 1227–1240.
33 Q. P. Cao, B. Liang, T. T. Tu, J. W. Wei, L. Fang and X. S. Ye, *RSC Adv.*, 2019, **9**, 5674–5681.
34 B. Liang, Q. P. Cao, X. Y. Mao, W. H. Pan, T. T. Tu, L. Fang and X. S. Ye, *IEEE Sens. J.*, 2021, **21**, 9642–9648.
35 A. Merkoci, *Paper Based Sensors*, Elsevier Science_Series, 2020.
36 K. Mahato, A. Srivastava and P. Chandra, *Biosens. Bioelectron.*, 2017, **96**, 246–259.
37 L. L. Shen, G. R. Zhang and B. J. M. Etzold, *ChemElectroChem*, 2020, **7**, 10–30.
38 K. Yamada, H. Shibata, K. Suzuki and D. Citterio, *Lab Chip*, 2017, **17**, 1206–1249.
39 P. Ma, S. Wang, J. Wang, Y. Wang, Y. Dong, S. Li, H. Su, P. Chen, X. Feng, Y. Li, W. Du and B.-F. Liu, *Anal. Chem.*, 2022, **94**, 13332–13341.
40 H. Martínez-Pérez-Cejuela, R. B. R. Mesquita, J. A. Couto, E. F. Simó-Alfonso, J. M. Herrero-Martínez and A. O. S. S. Rangel, *Talanta*, 2022, **250**, 123747.
41 A. W. Martinez, S. T. Phillips, M. J. Butte and G. M. Whitesides, *Angew. Chem., Int. Ed.*, 2007, **46**, 1318–1320.
42 A. Espinosa, J. Diaz, E. Vazquez, L. Acosta, A. Santiago and L. Cunci, *Talanta Open*, 2022, **6**, 100142.
43 S. Dortez, A. G. Crevillen and A. Escarpa, *Talanta*, 2023, **253**, 123914.
44 J. Wang, L. Zhang, X. Li, X. Zhang and H. Z. Yu, *RSC Adv.*, 2019, **9**, 23267–23275.
45 N. A. Meredith, C. Quinn, D. M. Cate, T. H. Reilly 3rd, J. Volckens and C. S. Henry, *Analyst*, 2016, **141**, 1874–1887.
46 K.-Y. Law, *J. Phys. Chem. Lett.*, 2014, **5**, 686–688.
47 A. W. Martinez, S. T. Phillips and G. M. Whitesides, *Proc. Natl. Acad. Sci. U. S. A.*, 2008, **105**, 19606–19611.
48 P. de Tarso Garcia, T. M. Garcia Cardoso, C. D. Garcia, E. Carrilho and W. K. Tomazelli Coltro, *RSC Adv.*, 2014, **4**, 37637–37644.
49 C. K. Camplisson, K. M. Schilling, W. L. Pedrotti, H. A. Stone and A. W. Martinez, *Lab Chip*, 2015, **15**, 4461–4466.
50 T. Lam, J. P. Devadhasan, R. Howse and J. Kim, *Sci. Rep.*, 2017, **7**, 1188.
51 W. Dungchai, O. Chailapakul and C. S. Henry, *Analyst*, 2011, **136**, 77–82.
52 E. M. Fenton, M. R. Mascarenas, G. P. Lopez and S. S. Sibbett, *ACS Appl. Mater. Interfaces*, 2009, **1**, 124–129.
53 J. J. Lu, S. G. Ge, L. Ge, M. Yan and J. H. Yu, *Electrochim. Acta*, 2012, **80**, 334–341.
54 B. Wongsing, A. Prakobkij, W. Anutrasakda and P. Jarujamrus, *Anal. Chem.*, 2022, **94**(40), 13785–13794.
55 S. Lee, D. S. Kulyk, S. O. Afriyie, K. Badu and A. K. Badu-Tawiah, *Anal. Chem.*, 2022, **94**(41), 14377–14384.
56 J. Y. Wang, M. R. N. Monton, X. Zhang, C. D. M. Filipe, R. Pelton and J. D. Brennan, *Lab Chip*, 2014, **14**, 691–695.
57 Y. F. Deng, Q. Z. Li, Y. H. Zhou and J. Qian, *ACS Appl. Mater. Interfaces*, 2021, **13**, 57084–57091.
58 P. D. Haller, C. A. Flowers and M. Gupta, *Soft Matter*, 2011, **7**, 2428–2432.
59 J. H. Lizama, H. Y. Tseng, Y. W. Shen and C. J. Chen, *Alexandria Eng. J.*, 2022, **61**, 7171–7181.
60 F. Ardakani, Z. Shojaeifard and B. Hemmateenejad, *Microchem. J.*, 2022, **181**, 107796.
61 L. Zhang, H. Kwok, X. Li and H. Z. Yu, *ACS Appl. Mater. Interfaces*, 2017, **9**, 39728–39735.
62 W. J. Paschoalino, S. Kogikoski, J. T. C. Barragan, J. F. Giarola, L. Cantelli, T. M. Rabelo, T. M. Pessanha and L. T. Kubota, *ChemElectroChem*, 2019, **6**, 10–30.
63 W. W. W. Hsiao, N. Sharma, T. N. Le, Y. Y. Cheng, C. C. Lee, D. T. Vo, Y. Y. Hui, H. C. Chang and W. H. Chiang, *Anal. Chim. Acta*, 2022, **1230**, 340389.
64 N. D. Duong, K. H. Nguyen-Phuoc, T. D. Mai-Hoang, K. Y. T. Do, T. B. Huynh, N. T. T. Nguyen, T. L. Tran and T. V. Hieu, *3 Biotech*, 2022, **12**(10), 243.
65 C. Turkcan, *Eur. Polym. J.*, 2022, **170**, 111162.
66 R. B. de Castro, A. C. A. de Souza, N. D. T. Pavione, J. V. B. de Moraes, I. C. Ribeiro, J. D. Agripino, G. C. Bressan, R. D. Vasconcellos, A. Silva and J. L. R. Fietto, *Anal. Biochem.*, 2022, **646**, 114648.
67 W. R. de Araujo and T. R. Paixao, *Analyst*, 2014, **139**, 2742–2747.
68 M. Santhiago, M. Strauss, M. P. Pereira, A. S. Chagas and C. C. Bufon, *ACS Appl. Mater. Interfaces*, 2017, **9**, 11959–11966.
69 A. C. Marques, L. Santos, M. N. Costa, J. M. Dantas, P. Duarte, A. Goncalves, R. Martins, C. A. Salgueiro and E. Fortunato, *Sci. Rep.*, 2015, **5**, 9910.
70 E. Yüzer, V. Doğan, V. Kılıç and M. Şen, *Sens. Actuators, B*, 2022, **371**, 132489.
71 W. J. Paschoalino, S. Kogikoski Jr., J. T. C. Barragan, J. F. Giarola, L. Cantelli, T. M. Rabelo, T. M. Pessanha and L. T. Kubota, *ChemElectroChem*, 2019, **6**, 10–30.
72 R. H. Muller and D. L. Clegg, *Anal. Chem.*, 1949, **21**, 1123–1125.
73 X. X. Yang, O. Forouzan, T. P. Brown and S. S. Shevkoplyas, *Lab Chip*, 2012, **12**, 274–280.
74 D. Sechi, B. Greer, J. Johnson and N. Hashemi, *Anal. Chem.*, 2013, **85**, 10733–10737.
75 H. Asano and Y. Shiraishi, *Anal. Chim. Acta*, 2015, **883**, 55–60.
76 J. L. Delaney, C. F. Hogan, J. F. Tian and W. Shen, *Anal. Chem.*, 2011, **83**, 1300–1306.
77 W. Liu, C. L. Cassano, X. Xu and Z. H. Fan, *Anal. Chem.*, 2013, **85**, 10270–10276.

78 L. Y. Ma, A. Nilghaz, J. R. Choi, X. Q. Liu and X. N. Lu, *Food Chem.*, 2018, **246**, 437–441.
79 W. Dungchai, O. Chailapakul and C. S. Henry, *Anal. Chem.*, 2009, **81**, 5821–5826.
80 Z. H. Nie, C. A. Nijhuis, J. L. Gong, X. Chen, A. Kumachev, A. W. Martinez, M. Narovlyansky and G. M. Whitesides, *Lab Chip*, 2010, **10**, 477–483.
81 L. Y. Shiroma, M. Santhiago, A. L. Gobbi and L. T. Kubota, *Anal. Chim. Acta*, 2012, **725**, 44–50.
82 P. Rattanarat, W. Dungchai, W. Siangproh, O. Chailapakul and C. S. Henry, *Anal. Chim. Acta*, 2012, **744**, 1–7.
83 E. Carrilho, A. W. Martinez and G. M. Whitesides, *Anal. Chem.*, 2009, **81**, 7091–7095.
84 A. W. Martinez, S. T. Phillips, B. J. Wiley, M. Gupta and G. M. Whitesides, *Lab Chip*, 2008, **8**, 2146–2150.
85 X. Li, J. F. Tian, T. Nguyen and W. Shen, *Anal. Chem.*, 2008, **80**, 9131–9134.
86 C. F. Yan, S. Y. Yu, Y. Jiang, Q. H. He and H. W. Chen, *Acta Chim. Sin.*, 2014, **72**, 1099–1104.
87 S. M. Wang, L. Ge, X. R. Song, J. H. Yu, S. G. Ge, J. D. Huang and F. Zeng, *Biosens. Bioelectron.*, 2012, **31**, 212–218.
88 Y. Lu, W. W. Shi, L. Jiang, J. H. Qin and B. C. Lin, *Electrophoresis*, 2009, **30**, 1497–1500.
89 X. Li, J. Tian, G. Garnier and W. Shen, *Colloids Surf., B*, 2010, **76**, 564–570.
90 E. Fu, B. Lutz, P. Kauffman and P. Yager, *Lab Chip*, 2010, **10**, 918–920.
91 K. M. Schilling, A. L. Lepore, J. A. Kurian and A. W. Martinez, *Anal. Chem.*, 2012, **84**, 3484–3484.
92 D. M. Cate, S. D. Noblitt, J. Volckens and C. S. Henry, *Lab Chip*, 2015, **15**, 2808–2818.
93 J. He, G. Xiao, X. Chen, Y. Qiao, D. Xu and Z. Lu, *RSC Adv.*, 2019, **9**, 23957–23963.
94 Z. Nie, F. Deiss, X. Liu, O. Akbulut and G. M. Whitesides, *Lab Chip*, 2010, **10**, 3163–3169.
95 T. Songjaroen, W. Dungchai, O. Chailapakul and W. Laiwattanapaisal, *Talanta*, 2011, **85**, 2587–2593.
96 L. Shen, J. A. Hagen and I. Papautsky, *Lab Chip*, 2012, **12**, 4240–4243.
97 N. Lopez-Ruiz, V. F. Curto, M. M. Erenas, F. Benito-Lopez, D. Diamond, A. J. Palma and L. F. Capitan-Vallvey, *Anal. Chem.*, 2014, **86**, 9554–9562.
98 J. A. Adkins, E. Noviana and C. S. Henry, *Anal. Chem.*, 2016, **88**, 10639–10647.
99 K. Song, R. Huang and X. Hu, *Micromachines*, 2021, **12**, 1391.
100 T. Li, B. Liang, Z. Ye, L. Zhang, S. Xu, T. Tu, Y. Zhang, Y. Cai, B. Zhang, L. Fang, X. Mao, S. Zhang, G. Wu, Q. Yang, C. Zhou, X. Cai and X. Ye, *Biosens. Bioelectron.*, 2022, **198**, 113855.
101 L. Ge, S. Wang, X. Song, S. Ge and J. Yu, *Lab Chip*, 2012, **12**, 3150–3158.
102 X. Wei, T. Tian, S. Jia, Z. Zhu, Y. Ma, J. Sun, Z. Lin and C. J. Yang, *Anal. Chem.*, 2015, **87**, 4275–4282.
103 X. Li and X. Liu, *Microfluid. Nanofluid.*, 2014, **16**, 819–827.
104 C. C. Tseng, C. T. Kung, R. F. Chen, M. H. Tsai, H. R. Chao, Y. N. Wang and L. M. Fu, *Sens. Actuators, B*, 2021, **342**, 130078.
105 A. W. Martinez, S. T. Phillips, G. M. Whitesides and E. Carrilho, *Anal. Chem.*, 2010, **82**, 3–10.
106 S. Nishat, A. T. Jafry, A. W. Martinez and F. R. Awan, *Sens. Actuators, B*, 2021, **336**, 129681.
107 V. Primpray, O. Chailapakul, M. Tokeshi, T. Rojanarata and W. Laiwattanapaisal, *Anal. Chim. Acta*, 2019, **1078**, 16–23.
108 A. K. Yetisen, M. S. Akram and C. R. Lowe, *Lab Chip*, 2013, **13**, 2210–2251.
109 G. C. Ilacas, A. Basa, K. J. Nelms, J. D. Sosa, Y. Liu and F. A. Gomez, *Anal. Chim. Acta*, 2019, **1055**, 74–80.
110 J. Ding, B. Li, L. Chen and W. Qin, *Angew. Chem., Int. Ed.*, 2016, **55**, 13033–13037.
111 G. M. Whitesides, *Nature*, 2006, **442**, 368–373.
112 J. L. Osborn, B. Lutz, E. Fu, P. Kauffman, D. Y. Stevens and P. Yager, *Lab Chip*, 2010, **10**, 2659–2665.
113 A. Böhm, F. Carstens, C. Trieb, S. Schabel and M. Biesalski, *Microfluid. Nanofluid.*, 2014, **16**, 789–799.
114 M. Li, L. Wang, R. Liu, J. Li, Q. Zhang, G. Shi, Y. Li, C. Hou and H. Wang, *Biosens. Bioelectron.*, 2021, **174**, 112828.
115 T. M. Squires, R. J. Messinger and S. R. Manalis, *Nat. Biotechnol.*, 2008, **26**, 417–426.
116 W. Guo, J. Hansson and W. van der Wijngaart, *Microsyst. Nanoeng.*, 2018, **4**, 2.
117 H. Darcy, *Les fontaines publiques de la ville de Dijon: Exposition et application des principes à suivre et des formules à employer dans les questions de distribution d'eau : Ouvrage terminé par un appendice relatif aux fournitures d'eau de plusieurs villes, au filtrage des eaux et à la fabrication des tuyaux de fonte, de plomb, de tôle et de bitume*, Victor Dalmont, Paris, 1856.
118 T. Shay, T. Saha, M. D. Dickey and O. D. Velev, *Biomicrofluidics*, 2020, **14**, 034112.
119 Q. Cao, B. Liang, X. Mao, J. Wei, T. Tu, L. Fang and X. Ye, *Electroanalysis*, 2021, **33**, 643–651.
120 M. Chung, G. Fortunato and N. Radacsi, *J. R. Soc., Interface*, 2019, **16**, 20190217.
121 V. Jain, M. Ochoa, H. Jiang, R. Rahimi and B. Ziaie, *Microsyst. Nanoeng.*, 2019, **5**, 29.
122 Z. Zhang, M. Azizi, M. Lee, P. Davidowsky, P. Lawrence and A. Abbaspourrad, *Lab Chip*, 2019, **19**, 3448–3460.
123 A. Vaquer, E. Baron and R. de la Rica, *ACS Sens.*, 2021, **6**, 130–136.
124 E. Cho, M. Mohammadifar and S. Choi, *Micromachines*, 2017, **8**, 265.
125 A. Vaquer, E. Baron and R. de la Rica, *ACS Sens.*, 2022, **7**, 488–494.
126 X. Weng, Z. Fu, C. Zhang, W. Jiang and H. Jiang, *Anal. Chem.*, 2022, **94**, 3526–3534.
127 S. Choi, S.-K. Kim, G.-J. Lee and H.-K. Park, *Sens. Actuators, B*, 2015, **219**, 245–250.

128 R. J. Maughan, *Eur. J. Clin. Nutr.*, 2003, **57**(Suppl 2), S19–S23.
129 A. Brueck, T. Iftekhar, A. B. Stannard, K. Yelamarthi and T. Kaya, *Sensors*, 2018, **18**, 1–22.
130 F. J. Zhao, M. Bonmarin, Z. C. Chen, M. Larson, D. Fay, D. Runnoe and J. Heikenfeld, *Lab Chip*, 2020, **20**, 168–174.
131 L. Wang, T. Xu, C. Fan and X. Zhang, *iScience*, 2021, **24**, 102028.
132 B. Zhong, K. Jiang, L. Wang and G. Shen, *Adv. Sci.*, 2022, **9**, e2103257.
133 S. Cinti, B. De Lellis, D. Moscone and F. Arduini, *Sens. Actuators, B*, 2017, **253**, 1199–1206.
134 T. Sun, J. Hui, L. Zhou, B. Lin, H. Sun, Y. Bai, J. Zhao and H. Mao, *Sens. Actuators, B*, 2022, **368**, 132184.
135 S. B. Kim, Y. Zhang, S. M. Won, A. J. Bandodkar, Y. Sekine, Y. Xue, J. Koo, S. W. Harshman, J. A. Martin, J. M. Park, T. R. Ray, K. E. Crawford, K. T. Lee, J. Choi, R. L. Pitsch, C. C. Grigsby, A. J. Strang, Y. Y. Chen, S. Xu, J. Kim, A. Koh, J. S. Ha, Y. Huang, S. W. Kim and J. A. Rogers, *Small*, 2018, **14**, e1703334.
136 Q. Li, H. Liu, S. Zhang, D. Zhang, X. Liu, Y. He, L. Mi, J. Zhang, C. Liu, C. Shen and Z. Guo, *ACS Appl. Mater. Interfaces*, 2019, **11**, 21904–21914.
137 X. Mu, X. Xin, C. Fan, X. Li, X. Tian, K. F. Xu and Z. Zheng, *Chem. Commun.*, 2015, **51**, 6365–6368.
138 S. Emaminejad, W. Gao, E. Wu, Z. A. Davies, H. Yin Yin Nyein, S. Challa, S. P. Ryan, H. M. Fahad, K. Chen, Z. Shahpar, S. Talebi, C. Milla, A. Javey and R. W. Davis, *Proc. Natl. Acad. Sci. U. S. A.*, 2017, **114**, 4625–4630.
139 S. N. Cheuvront, R. Carter 3rd and M. N. Sawka, *Curr. Sports Med. Rep.*, 2003, **2**, 202–208.
140 H. Y. Y. Nyein, M. Bariya, L. Kivimaki, S. Uusitalo, T. S. Liaw, E. Jansson, C. H. Ahn, J. A. Hangasky, J. Zhao, Y. Lin, T. Happonen, M. Chao, C. Liedert, Y. Zhao, L. C. Tai, J. Hiltunen and A. Javey, *Sci. Adv.*, 2019, **5**, eaaw9906.
141 P. Pirovano, M. Dorrian, A. Shinde, A. Donohoe, A. J. Brady, N. M. Moyna, G. Wallace, D. Diamond and M. McCaul, *Talanta*, 2020, **219**, 121145.
142 S. Y. Oh, S. Y. Hong, Y. R. Jeong, J. Yun, H. Park, S. W. Jin, G. Lee, J. H. Oh, H. Lee, S. S. Lee and J. S. Ha, *ACS Appl. Mater. Interfaces*, 2018, **10**, 13729–13740.
143 S. Nishat, A. T. Jafry, A. W. Martinez and F. R. Awan, *Sens. Actuators, B*, 2021, **336**, 129681.
144 W. Gao and D. Wen, *View*, 2021, **2**, 20200124.
145 G. Li, J. Hao, W. Li, F. Ma, T. Ma, W. Gao, Y. Yu and D. Wen, *Anal. Chem.*, 2021, **93**, 14068–14075.
146 T. Li, Z. Ye, Y. Cai, T. Tu, B. Zhang, S. Zhang, L. Fang, X. Mao, S. Xu, X. Ye and B. Liang, *J. Electroanal. Chem.*, 2022, **911**, 116183.
147 M. Amjadi, K. U. Kyung, I. Park and M. Sitti, *Adv. Funct. Mater.*, 2016, **26**, 1678–1698.
148 X. Zhao, H. Wu, B. L. Guo, R. N. Dong, Y. S. Qiu and P. X. Ma, *Biomaterials*, 2017, **122**, 34–47.
149 T. T. Tu, B. Liang, S. S. Zhang, T. Y. Li, B. Zhang, S. Y. Xu, X. Y. Mao, Y. Cai, L. Fang and X. S. Ye, *Adv. Funct. Mater.*, 2021, **31**, 2101374.
150 P. Chandra and R. Prakash, *Nanobiomaterial Engineering*, Springer, Singapore, 2020.
151 Y. Y. Yang, E. Noviana, M. P. Nguyen, B. J. Geiss, D. S. Dandy and C. S. Henry, *Anal. Chem.*, 2017, **89**, 71–91.